공학석사학위논문

보행자 거동 및 운전자 주행 특성 기반의 자율주행 종방향 거동 계획

Human-like Longitudinal Motion Planning in Consideration of Pedestrian Behavior Characteristics for Urban Autonomous Driving

2020년 8월

서울대학교 대학원

기계공학부

김 유 진

Abstract

Human-like Longitudinal Motion Planning in Consideration of Pedestrian Behavior Characteristics for Urban Autonomous Driving

Yujin Kim

School of Mechanical Engineering

The Graduate School

Seoul National University

This paper presents a pedestrian model considering uncertainty in the direction of future movement and a human-like longitudinal motion planning algorithm for autonomous vehicle in the interaction situation with pedestrians. Interactive driving with pedestrians is essential for autonomous driving in urban environments. However, interaction with pedestrians is very challenging for autonomous vehicle because it is difficult to predict movement direction of pedestrians. Even if there exists uncertainty of the behavior of pedestrians, the autonomous vehicles should

plan their motions ensuring pedestrian safety and respond smoothly to pedestrians. To implement this, a pedestrian probabilistic yaw model is introduced based on behavioral characteristics and the human driving parameters are investigated in the interaction situation. The paper consists of three main parts: the pedestrian model definition, collision risk assessment based on prediction and human-like longitudinal motion planning. In the first section, the main key of pedestrian model is the behavior tendency with correlation between pedestrian's speed and direction change. The behavior characteristics are statistically investigated based on perceived pedestrian tracking data using light detection and ranging(Lidar) sensor and front camera. Through the behavior characteristics, movement probability for all directions of the pedestrian is derived according to pedestrian's velocity. Also, the effective moving area can be limited up to the valid probability criterion. The defined model allows the autonomous vehicle to know the area that pedestrian may head to a certain probability in the future steps. This helps to plan the vehicle motion considering the pedestrian yaw state's uncertainty and to predetermine the motion of autonomous vehicle from the pedestrians who may have a risk. Secondly, a risk assessment is required and is based on the pedestrian model. The dynamic states of pedestrians and subject vehicle are predicted to do a risk assessment. In this section, the pedestrian behavior is predicted under the assumption of moving to the most dangerous direction in the effective moving area obtained above. The prediction of vehicle behavior is performed using a lane keeping model in which the vehicle follows a given path. Based on the prediction result, it is checked whether there will be a collision between the pedestrian and the vehicle if deceleration motion is not taken. Finally, longitudinal motion planning is

determined for target pedestrians with possibility of collision. Human driving data is first examined to obtain a proper longitudinal deceleration and deceleration starting point in the interaction situation with pedestrians. Several human driving parameters are defined and applied in determining the longitudinal acceleration of the vehicle. The longitudinal motion planning algorithm is verified via vehicle tests. The test results confirm that the proposed algorithm shows similar longitudinal motion and deceleration decision to a human driver based on predicted pedestrian model.

Keyword: Autonomous Driving, Longitudinal Motion Planning, Probabilistic Pedestrian Model, Human-Like Driving

Student Number: 2018-20946

Contents

List of Figures

List of Tables

Chapter 1

Introduction

1.1. Background and Motivation

The Advanced Driver Assistance System(ADAS), which helps drivers to drive safely before reaching fully autonomous driving technology, is widely used and research is underway to expand the technology area. Currently, the development of autonomous highway driving technology had progressed above a certain level and it aims to realize autonomous driving in the urban environment.

The main issue of autonomous urban driving is driving safely, interacting with various types of objects or pedestrians using the road. Among various road users, such as bicycles, segways, motorcycles, vehicles and pedestrians, pedestrians are the most vulnerable users who can be seriously injured in an accident.

The Euro New Car Assessment Program(NCAP) has added ‘AEB pedestrian’ as a safety assessment item for active safety systems since 2016. Furthermore, the pedestrian safety issue was raised again when a pedestrian death accident occurred by the Uber’s autonomous vehicle in 2018. Hence, the technology to secure pedestrian safety is essential to the advent of the era of fully autonomous vehicles in urban environments.

To do so, it is necessary for autonomous vehicle to predict pedestrian movement and perform proactive motion. However, it is difficult for autonomous vehicles to accurately model and predict pedestrian movements because pedestrians are free to switch their movement directions. In addition, depending on the sensor configuration of the vehicle, there may be a limitation in obtaining pedestrian information and all contextual information from the surrounding environment in real-time.

To implement autonomous driving for pedestrians considering above problems, this study focuses on deriving the movement characteristics of pedestrians using only fundamental states, such as position, velocity and yaw. Also, in order to smoothly realize interactive driving with pedestrians, human driving characteristics are investigated and applied to determine vehicle's motion. The main target of this research is to define future movement region for each pedestrian in real time and implement human-like longitudinal motion planning. This study can realize autonomous driving to secure pedestrian safety and plan proper vehicle motion according to situation.

1.2. Previous Researches

The areas of research related to pedestrians required for autonomous driving technology largely consist of pedestrian model definition, movement prediction, and interactive motion between pedestrian and vehicle.

The following studies have been conducted on pedestrian modeling and path prediction. Yoriyoshi Hashimoto[1][2] applied Dynamic Bayesian Network (DBN) model based on contextual information which includes traffic signal, surround vehicle, group situation and crosswalk length. The information is obtained using a camera sensor. N. Schneider[3] proposed pedestrian path prediction using Interacting Multiple Models (IMM) with three basic motions such as constant velocity, acceleration and turn. Julian F.P.Kooij[4] presented a path prediction of vulnerable road user (VRU) using combination of basic motion switching model and context information including line of gaze and road infrastructure. In addition, various researches have been studied to estimate the pedestrian's intention from information such as the face direction, several body languages and leg motion using vision sensors[5] [6] [7].

Several studies have been conducted to analyze the driving characteristics of the human driver in the interaction situation with pedestrians. Tomas Bertulis[8] investigated the correlation between driver approach speed and yielding rates to pedestrians. Friederike Schneemann[9] analyzed the actual driver's interaction on the crosswalks, which includes the driver's reaction time for vehicle speed and driver's stochastic strategy. Yanlei Gu[10] proposed gap acceptance model for a human-like motion planning in the left-turning situation. Also, Ya-Chuan[11] Hsu

used an Markov Decision Process with risk minimizing reward model to express the interaction between a pedestrian and a vehicle. Markkula.G[12] define the behavior model of driver and pedestrian in certain scenarios. Some studies research pedestrian walking behavior such as speed and crossing decision[13][14][15].

In order to respond to pedestrians for autonomous driving in the urban environment, studies in the three fields above should be comprehensively applied. In this study, a specific situation is not limited considering the fundamental state information of pedestrian, not a model that assumes constant yaw, constant acceleration, etc. In addition, since it uses only basic Lidar tracking information, so it has less load to handle and can be applied in real time as the autonomous vehicle is driving.

Furthermore, above rule-based pedestrian path prediction sometimes tends to have fairly large prediction errors due to multiple assumptions and pedestrian movement characteristics that easily change their motion. In this study, pedestrian safety can be ensured by defining a behavior uncertainty region beyond a certain probability instead of path prediction. The interaction between the vehicle and the pedestrian was implemented by applying important factors derived by examining the driving data of the human driver to the deceleration plan.

1.3. Thesis Objective and Outline

This study aims to define the area in which pedestrians can behave in the future, and to enable autonomous vehicles to behave like humans in the presence situation of pedestrians. There is a limitation in accurately predicting the changeable behavior of a pedestrian. It is also difficult to obtain all the contextual information of situation in real-time while the autonomous vehicle is driving, depending on the sensor configuration and processing speed of the autonomous vehicle.

To achieve the goal with a limited information, the overall algorithm consists of three main parts: the pedestrian model definition using pedestrian's dynamic movement characteristics, prediction-based collision risk assessment and human-like longitudinal motion planning through accumulated human driving data.

In the first part, the pedestrian model and the region of pedestrian's future movement is defined using derived behavior characteristics from accumulated pedestrian state data. Pedestrian's state information is obtained using IBEO Lidar sensors and front camera mounted on the vehicle. Through the investigated state information, the correlation between pedestrian speed and direction change is identified and it is used to derive the possibility of pedestrian movement in all directions. The effective range of future movement direction is defined using the derived possibility. Also, the radius of region reflects the velocity of pedestrian.

In the second part, vehicle and pedestrian movement behavior predictions are conducted for risk assessment. The movement prediction of pedestrian is assumed to maintain the current speed and behave in the direction of the highest collision risk within the region derived above. Vehicle movement prediction uses a lane

keeping model that assumes the vehicle follows a given local path. The desired yaw rate is derived through the lane keeping behavior model and applied as a virtual measurement in the extended Kalman filter(EKF), which is prediction method. As a result of the prediction, if the predicted behavior range of the vehicle and the target pedestrian overlaps within the time horizon, the risk existence is confirmed.

Finally, the longitudinal motion of the vehicle is determined considering the future movement in the presence situation of pedestrians. In order to realize a human-like longitudinal movement of the vehicle, human driving data is collected and critical elements is defined as human driving parameters. These parameters are applied to calculate longitudinal acceleration. Furthermore, the driving mode is defined through analyzing the human data, which is soft and hard mode. The hard mode is conceptually a case that stopping the vehicle is inevitable, and soft mode is when the vehicle passes smoothly after gentle deceleration without stopping. The driving mode and acceleration are selected by relative distance and velocity.

The result of applying the algorithm to the autonomous vehicle is compared with the driving of the human driver in the same situation. The results demonstrate that the starting time of deceleration and the time trajectory of Time-To-Collision(TTC) and clearance are similar.

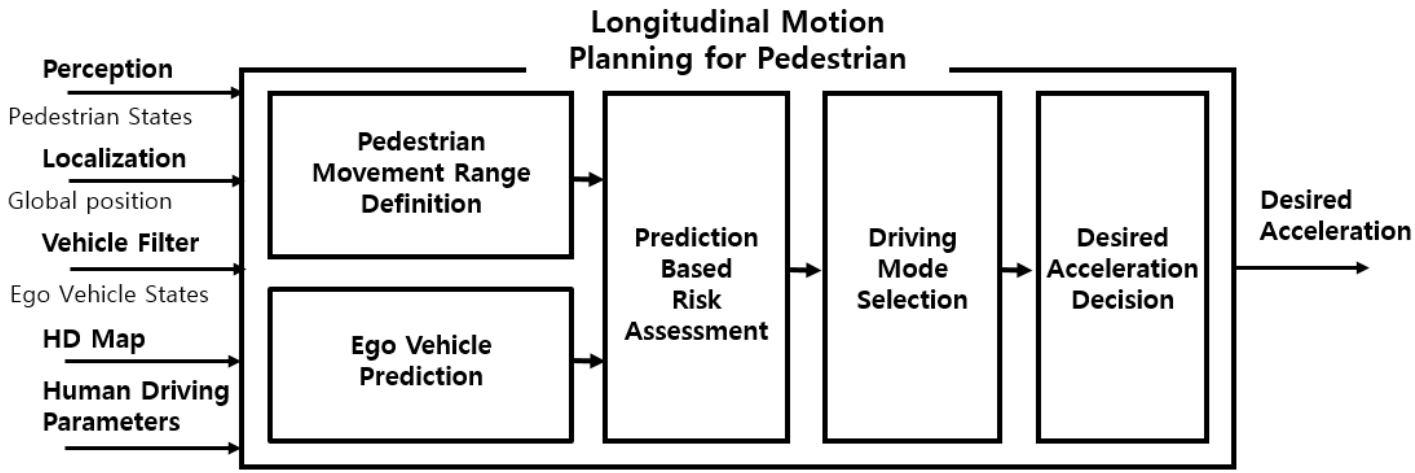

Fig. 1 System overview of proposed longitudinal motion planning algorithm for pedestrians.

Chapter 2

Probabilistic Pedestrian Yaw Model

In this section, the behavioral characteristics of pedestrians are investigated and a pedestrian model is derived based on investigated results. Pedestrians can freely change the direction of movement in all directions, unlike the movement of other road users such as vehicles or motorcycles. Nevertheless, in order for autonomous vehicle to drive in urban environment, it is necessary to determine the behavior of the vehicle by predicting pedestrian behavior. If the movement of pedestrians is considered in all directions, the motion of autonomous vehicle will be excessively conservative than necessary. Hence, additional information is needed to indicate the tendency of pedestrian behavior. The information that can be obtained is various depending on the sensor configuration, but in this study, the behavior of the pedestrian is analyzed with only the fundamental state information such as position, velocity, acceleration and yaw. To characterize pedestrian behavior, the 5000-step datasets of pedestrian state were collected on campus at the Seoul National University. Data was obtained by the in-vehicle IBEO Lidar sensor, at frequency of 25Hz.

2.1. Pedestrian Behavior Characteristics

The main feature of pedestrian behavior in this study is the correlation between movement speed and direction change. The feature is verified by the measured pedestrian datasets. Fig. 2(a) shows the distributions of yaw angle change between current step[k] and last time step[k-1] for each specific speed section of the pedestrian. The standard deviation can be obtained by fitting dataset to Gaussian distribution. Fig. 2(b) shows the same data in the yaw angle change and velocity plane. The graph shows a specific tendency between the velocity and the standard deviation of distribution. As the velocity increases, the standard deviation of distribution decreases, as illustrated in the Fig. 2. This means that fast-moving pedestrians are more likely to maintain their current direction of movement, while slow-moving pedestrians tend to alter directions. The feature can be used to define probabilistic movement range of pedestrian for a certain time horizon.

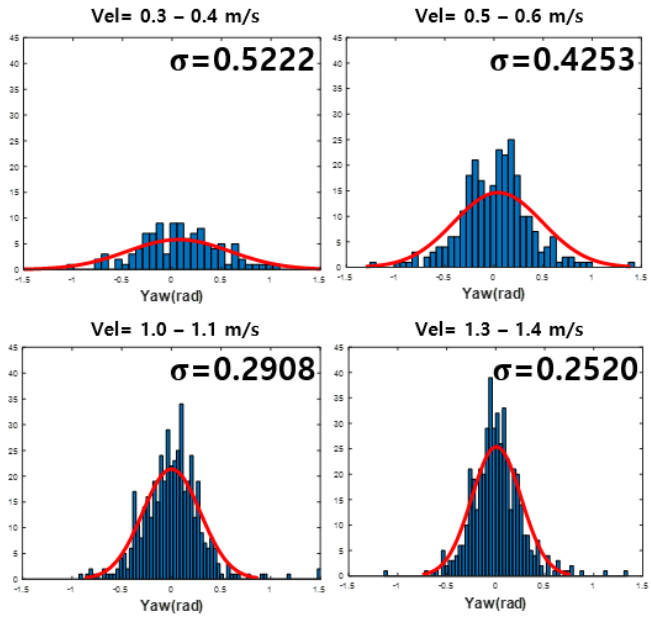

(a) Gaussian distributions of yaw angle change according to velocity

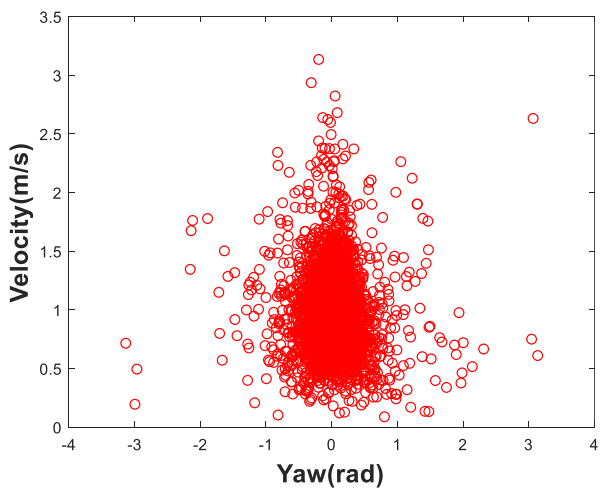

(b) Distribution between yaw angle change and yaw angle

Fig. 2 Distribution of pedestrian movement data

2.2. Probabilistic Movement Range

The standard deviation tends to be inversely proportional to the pedestrian velocity, as illustrated in the Fig. 2. The relations can be formulated as follows through cumulated datasets. Equation (1) between the standard deviation and speed is obtained using MATLAB Curve Fitting Toolbox.

$$\sigma = \frac{0.03889}{v^{2.36}} + 0.2659 \tag{1}$$

Fig. 3 shows the fitted relationship in the x-y plane. According to this formula, each pedestrian has a certain probability in all movement directions depending on their speed. To define effective movement range, the yaw angle limit is set to ±1.5 sigma representing 86.7% through a heuristic method. In addition, the radius of the moving range is determined as a predicted position assuming a constant velocity during a certain time horizon. The time horizon is determined 6 sec using maximum perception distance(50m) and minimum velocity in the urban environment(30kph). In the case of a stationary pedestrian, there is a probability in all directions, and the radius of the range is set to a certain value in consideration of the human stride.

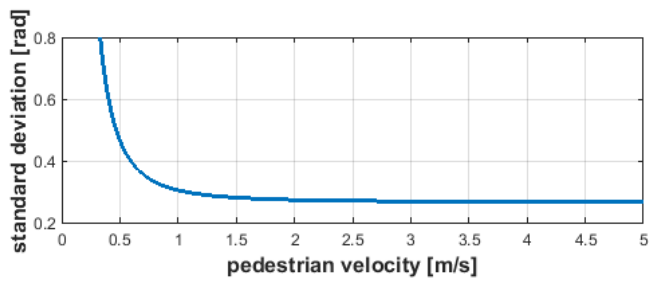

Fig. 3 Standard deviation of yaw angle change distribution according to pedestrian velocity

In addition, the movement range based on probabilistic pedestrian yaw model is used to select target pedestrians that need attention. Target pedestrians are selected by checking whether the ranges overlap with driving lane of ego vehicle based on high-definition(HD) map. The conceptual image is shown in the Fig. 4.

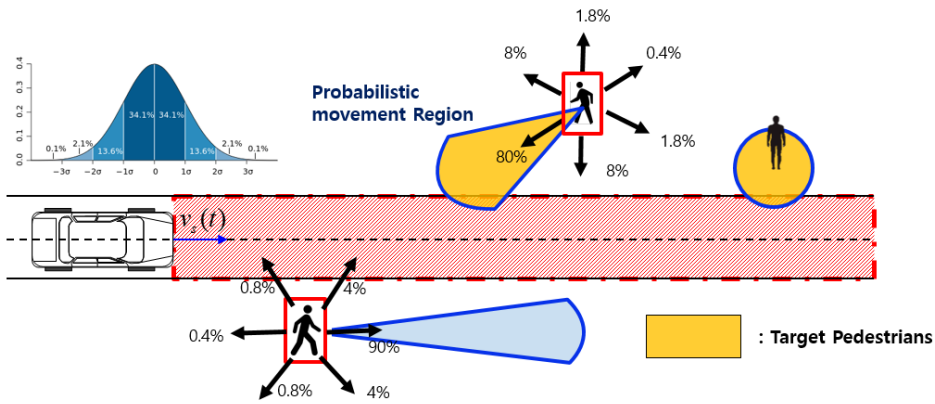

Fig. 4 Visualization of probabilistic pedestrian yaw model

Chapter 3

Prediction Based Risk Assessment

When pedestrians cross the road, the movement direction of vehicles and pedestrians is usually almost perpendicular. Hence, the collision risk is assessed considering not only relative longitudinal distance and TTC, but also lateral behavior with time term. This is because pedestrians might pass through the driving lane before a collision occurs even though there is a sufficient danger of collision in the longitudinal direction. Therefore, the time series trajectory of the vehicle and the pedestrian should be predicted. If the two predicted trajectories overlap, the risk is judged. In addition, the prediction enables proactive motion of vehicle. It can increase the vehicle's safe speed range to cope with pedestrians crossing. The safe speed range and safe zone based on prediction are analyzed in the section 3.3.

Pedestrian trajectory prediction is assumed to move in the direction with the highest risk within the effective yaw range derived above. Also, it is assumed that the pedestrian maintains the current speed. Under the assumptions, it is possible to obtain the two-dimensional trajectory of the pedestrian until the time at which the target pedestrian leaves the driving lane.

To predict the future behavior of the subject vehicle, the lane keeping behavior model is used that assumes the subject vehicle maintains the current driving lane. Then, the desired yaw rate based on the lane keeping behavior model is applied as

a virtual measurement in the extended Kalman filter(EKF), which is prediction method. This section is mainly referenced from [16] and [17]. The conceptual image is shown in the Fig.5.

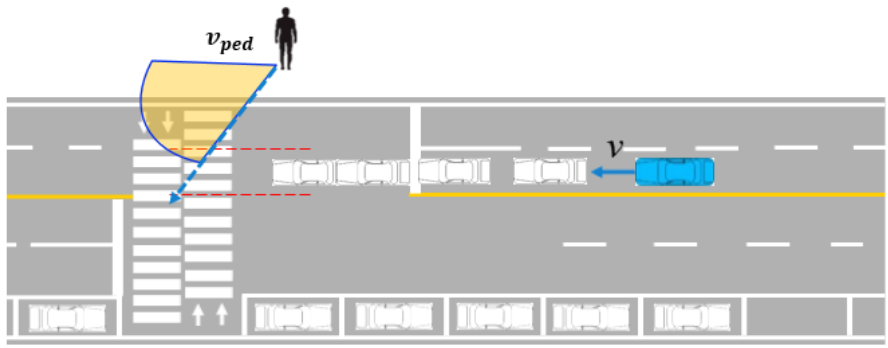

Fig. 5 Concept of prediction for pedestrian and subject vehicle

3.1. Lane Keeping Behavior Model

The lane keeping behavior model uses a dynamic model with lateral position error and angular error states with respect to the current lane. The current lane information is obtained from the in-vehicle GPS sensor and HD map. It is curve-fitted as the 2nd order polynomial. The error states are defined in inertial fixed coordinates and each error and differential term are as shown in equation (4)-(7).

$$e_y = p_y - (a_2 \cdot p_x^{\,2} + a_1 \cdot p_x + a_0) \tag{4}$$

$$\begin{aligned} \dot{e}_y &= \frac{d}{dt}(p_y) - \frac{d}{dp_x}(a_2 \cdot p_x^{\,2} + a_1 \cdot p_x + a_0) \cdot \frac{d}{dt}(p_x) \\ &\cong v\sin\theta - (2a_2 \cdot p_x + a_1) \cdot v\cos\theta \end{aligned} \tag{5}$$

$$\begin{aligned} e_\theta &= \theta - \tan^{-1}\left(\frac{d}{dp_x}(a_2 \cdot p_x^{\,2} + a_1 \cdot p_x + a_0)\right) \\ &= \theta - \tan^{-1}(2a_2 \cdot p_x + a_1) \end{aligned} \tag{6}$$

$$\begin{aligned} \dot{e}_\theta &= \dot{\theta} - \frac{d}{dt}\{\tan^{-1}(2a_2 \cdot p_x + a_1)\} \\ &= \gamma - \frac{1}{1 + (2a_2 \cdot p_x + a_1)^2} \cdot \frac{d}{dt}(2a_2 \cdot p_x + a_1) \\ &= \gamma - \frac{2a_2}{1 + (2a_2 \cdot p_x + a_1)^2} \cdot (v\cos\theta) \\ &\cong \gamma - 2a_2 \cdot (v\cos\theta) \end{aligned} \tag{7}$$

where p_x is the vehicle's longitudinal position, p_y is the vehicle's lateral position, θ is heading angle and v is the longitudinal velocity of the subject vehicle. If the yaw rate error term can be assumed as a 1st-order system with system

input of the desired yaw rate, it is expressed as equation (8).

$$\dot{e}_{\gamma} = f(\gamma - \gamma_{des}) \tag{8}$$

Above equations can be represented by the state-space equation as in equation (9).

$$\begin{aligned}\dot{x}_e &= F_e \cdot x_e + G_e \cdot \gamma_{des} + G_w \cdot a_2 \\ &= \begin{bmatrix} 0 & v\cos\theta & 0 \\ 0 & 0 & 1 \\ 0 & 0 & f \end{bmatrix} \cdot \begin{bmatrix} e_y \\ e_\theta \\ \gamma \end{bmatrix} + \begin{bmatrix} 0 \\ 0 \\ -f \end{bmatrix} \cdot \gamma_{des} + \begin{bmatrix} 0 \\ -2v\cos\theta \\ 0 \end{bmatrix} \cdot a_2\end{aligned}$$

Also, γ_{des} denotes the desired yaw rate. This can be set by state feedback and a feed-forward terms to converge error into zero, which is shown in equation (10).

$$\gamma_{des} = -\begin{bmatrix} c_1 & c_2 & c_3 \end{bmatrix} \cdot x_e + \gamma_{ff} \tag{10}$$

The feedback gains are decided through pole-place method, and the feed-forward term γ_{ff} is simply calculated to generate zero errors using above equation.

$$\gamma_{ff} = 2a_2 v\cos\theta(c_3 + 1) \tag{11}$$

As mentioned, the derived γ_{des} is used as a virtual measure in EKF prediction.

3.2. Subject Vehicle Prediction

The extended Kalman filter is used to predict states of the Ego vehicle. The process model can be described via Taylor Methods as below.

$$
\begin{aligned}
x_p &= \begin{bmatrix} p_{x,p} & p_{y,p} & \theta_p & v_p & \gamma_p & a_p & \dot{\gamma}_p \end{bmatrix}^T \\
x_p[i+1] &= f_p\left(x_p[i+1]\right) + w_p[i] \\
&= \begin{bmatrix} f_{1,p} & f_{2,p} & f_{3,p} & f_{4,p} & f_{5,p} & f_{6,p} & f_{7,p} \end{bmatrix}^T + w_p[i]
\end{aligned}
\tag{12}
$$

where

$$\mathbf{f_{1,p}} = p_{x,p} + \left(v_p \cos\theta_p\right)\Delta t + \left(a_p \cos\theta_p + \gamma_p v_p \sin\theta_p\right)\frac{\Delta t^2}{2}$$

$$\mathbf{f_{2,p}} = p_{y,p} + \left(v_p \sin\theta_p\right)\Delta t + \left(a_p \sin\theta_p + \gamma_p v_p \cos\theta_p\right)\frac{\Delta t^2}{2}$$

$$\mathbf{f_{3,p}} = \theta_p + \left(\gamma_p\right)\Delta t + \left(\dot{\gamma}_p\right)\frac{\Delta t^2}{2}$$

$$\mathbf{f_{4,p}} = v_p + \left(a_p\right)\Delta t$$

$$\mathbf{f_{5,p}} = \gamma_p + \left(\dot{\gamma}_p\right)\Delta t$$

$$\mathbf{f_{6,p}} = a_p$$

$$\mathbf{f_{7,p}} = \dot{\gamma}_p$$

$$\mathbf{F_p}[i] = \left.\frac{\partial \mathbf{f_p}}{\partial \mathbf{x_p}}\right|_{\mathbf{x_p}=\hat{\mathbf{x}}_\mathbf{p}[i]}$$

$$\mathbf{B_p} = \begin{bmatrix} 0 & 0 & 0 & 0 & 0 & 0 & 1 \\ 0 & 0 & 0 & 0 & 0 & 1 & 0 \end{bmatrix}^T$$

$$\mathbf{w_p}[i] \sim \left(0, \mathbf{W_p}[i]\right)$$

$$\mathbf{W_p}[i] = \left(\mathbf{B_p}\Delta t + \mathbf{F_p}[i]\mathbf{B_p}\frac{\Delta t^2}{2}\right)\mathbf{Q_p}\left(\mathbf{B_p}\Delta t + \mathbf{F_p}[i]\mathbf{B_p}\frac{\Delta t^2}{2}\right)^T$$

where $p_{x,p}, p_{x,p}, \theta_p$ denote the predicted x, y position and yaw angle in the body-fixed coordinates, setting zero values as initial value. $v_p, \gamma_p, a_p, \dot{\gamma}_p$ are the

predicted longitudinal velocity, yaw rate, longitudinal acceleration and yaw acceleration, respectively. The initial values of these four states are obtained by chassis sensor in the vehicle. N_p is the length of the prediction horizon and is determined by the estimated time for the target pedestrian to complete crossing the driving lane of ego vehicle. Also, the derivative terms of acceleration and yaw rate are assumed as zero value.

The measurement model of EKF estimator can be described using the desired yaw rate as virtual measurement.

$$\begin{aligned}\mathbf{z_p}[i] &= \mathbf{H_p}\mathbf{x_p}[i] + \mathbf{v_p}[i] \\ &= \begin{bmatrix}0 & 0 & 0 & 0 & 1 & 0 & 0\end{bmatrix} x_p[i] + v_p[i] \\ &= \hat{\gamma}_{des,p}[i] \\ &= -\mathbf{C}\cdot\bar{\mathbf{x}}_{\mathbf{e,p}}[i] + \gamma_{ff}[i]\end{aligned} \tag{13}$$

where

$$\begin{aligned}\bar{\mathbf{x}}_{\mathbf{e,p}}[i] &= \mathbf{f_e}\left(\bar{\mathbf{x}}_{\mathbf{p}}[i],\ \hat{\mathbf{x}}_{\mathbf{r}}[0]\right) \\ &= \begin{bmatrix}\bar{e}_y[i] & \bar{e}_\theta[i] & \bar{\gamma}_p[i]\end{bmatrix}^T \\ &= \begin{bmatrix} \bar{p}_{y,p}[i] - \left\{\hat{a}_2\cdot\bar{p}_{x,p}[i]^2 + \hat{a}_1\cdot\bar{p}_{x,p}[i] + \hat{a}_0\right\} \\ \bar{\theta}_p[i] - \tan^{-1}\left(\hat{a}_2\cdot\bar{p}_{x,p}[i] + \hat{a}_1\right) \\ \bar{\gamma}_p[i]\end{bmatrix}\end{aligned}$$

$$\mathbf{v_p}[i] \sim (0, \mathbf{V_p}[i])$$

$$\mathbf{V_p} = \mathbf{V_{p,const}} + \begin{bmatrix}\bar{e}_y[i] & \bar{e}_\theta[i]\end{bmatrix}\mathbf{W_{correct}}\begin{bmatrix}\bar{e}_y[i] & \bar{e}_\theta[i]\end{bmatrix}^T$$

where $W_{correct}$ indicates the additional covariance of the desired yaw rate. By iteratively applying the extended Kalman filter using the above process and measurement model, the longitudinal and lateral trajectory of the ego vehicle can be predicted during the time horizon.

3.3. Safety Region Based on Prediction

Safety region that can be secured through prediction are investigated. First of all, the maximum perception distance should be analyzed to obtain safety region. Depending on the clearance, the number of Lidar points reflected by a pedestrian is analyzed based on the 4-channel IBEO Lidar sensor with resolution 5°. It is calculated for each adult and child as shown in the Table1 below.

Distance	**Adult**(1700*600mm)	**Child**(1200*400mm)
3m	~184	~122
10m	~56	~36
30m	~18	~6
40m	~12	~5
50m	~6	~4
60m	~3	~2(EA)

Table1. The number of IBEO Lidar points for adult and child pedestrian

In order to classify and track pedestrian reliably, more than 3 points must be secured, so the perception distance limit(S_{lim}) is about 50m. The longitudinal distance($s_{required}$) required to avoid collision can be calculated by equation (14). T_{delay} is the sum of system delay and process delay, which is set to 1.2sec in this study. $a_{\min}$ is the minimum acceleration(maximum deceleration) of general situation and is set to $-3m/s^2$ in this study. Considering S_{lim} value, the maximum safety velocity($V_{\max}$) is about 50kph.

$$s_{required} = v_{veh} T_{delay} + \frac{v^2}{2|a_{\min}|} \tag{14}$$

Assuming that only the current position of the pedestrian without prediction is considered, the deceleration starting clearance of the subject vehicle can be calculated according to lateral distance(s_{lat}) of recognized pedestrian from equation (15). The conceptual image is shown in the Fig.6.

$$C_{start} = S_{\lim} - v_{veh} \cdot \frac{s_{lat}}{v_{ped}} \tag{15}$$

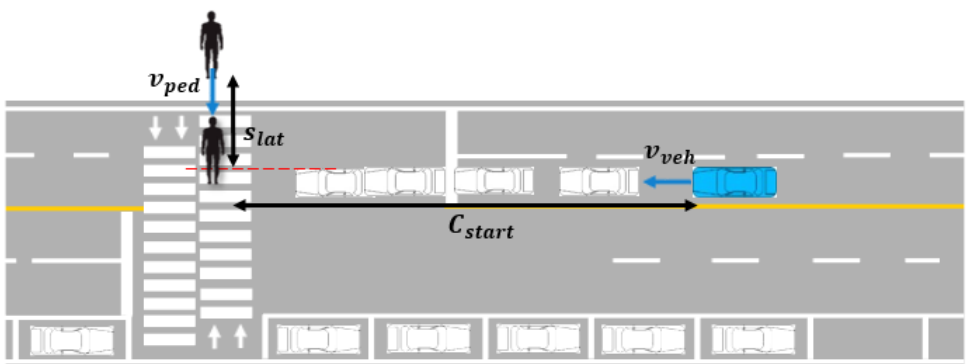

Fig. 6 Concept of prediction parameters

If the v_{ped} is set to the pedestrian's average velocity $1.3m/s^2$[13], Fig.7 shows $s_{required}$ and C_{start} according to the s_{lat}. Each crossing point means the maximum velocity that avoids to collision without prediction. Also, the region that needs prediction can be presented in the s_{lat} and velocity plane, as shown red zone in Fig.8. The baseline of Fig.10 is calculated by the equation (16).

$$s_{lat} = v_{ped}\left(\frac{S_{\lim}}{v_{veh}} - \frac{v_{veh}}{2|a_{\min}|} - T_{delay}\right) \tag{16}$$

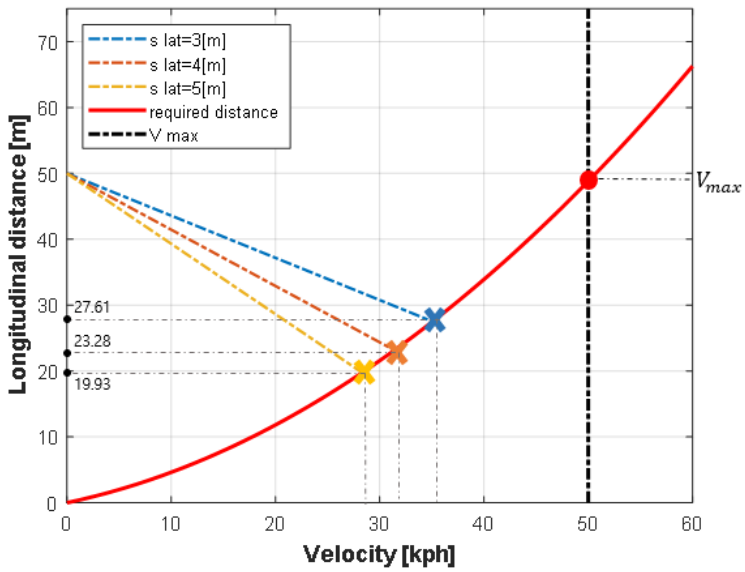

Fig. 7 Required distance and deceleration starting distance according to lateral distance

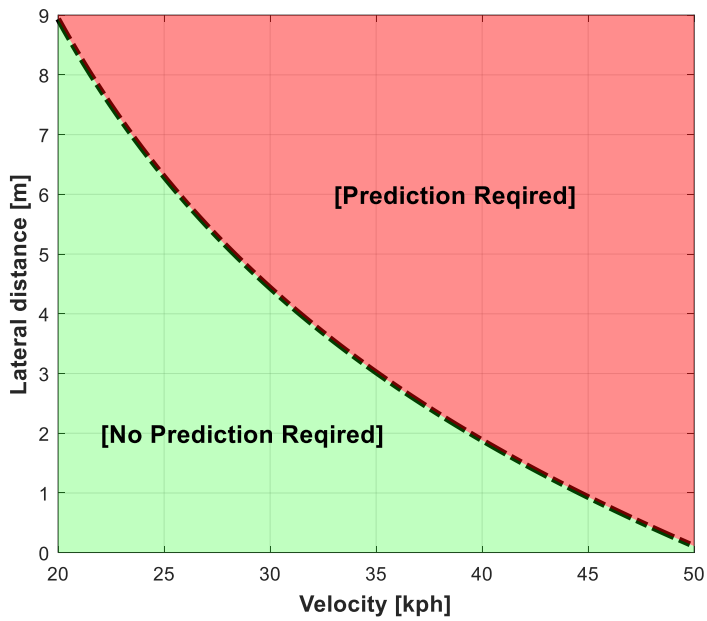

Fig. 8 Prediction required region in the lateral distance and velocity plane

Chapter 4

Human-like
Longitudinal Motion Planning

4.1. Human Driving Parameters Definition

Before determining the subject vehicle's motion for the target pedestrians, the critical driving elements are analyzed to realize the human-like driving in the pedestrian presence situation. In order to define human driving parameters, the driving data of experienced drivers is collected by circular driving on campus at the Seoul National University. Also, the data is obtained by in-vehicle Lidar sensor and vehicle chassis sensor.

According to human driving data, the vehicle's motion can be roughly divided into two modes. One case is when stopping the vehicle is inevitable (hard mode), and the other is when the vehicle passes smoothly after gentle deceleration without stopping (soft mode), which happens more frequently. The human driving parameters are defined in each driving mode. The parameter values are determined as the average value of cumulative human driving data and are shown in Table2.

4.1.1. Hard Mode Distance

The distance parameter of the hard mode is a proper minimum distance that pedestrians and driver do not feel threatened when stopping, denoted as d_{hard}. In other words, it is the clearance to be secured when vehicle stops due to pedestrians.

4.1.2. Soft Mode Distance and Velocity

The distance parameter of the soft mode is the clearance between the vehicle and the pedestrian at the time the pedestrian completes crossing, denoted as d_{soft}. The velocity parameter of the soft mode is the vehicle velocity at the same point, denoted as v_{soft}.

4.1.3. Time-To-Collision

TTC, as is well known, is the value obtained by dividing the relative distance by the relative speed. In this study, two TTCs are defined and applied. One is the TTC at the time of starting deceleration, denoted as TTC_{decel}. The other is TTC at the time the pedestrian completes crossing, denoted as TTC_{soft}. This parameter is obtained using d_{soft} and v_{soft} at the same point.

Human Driving Parameter	Average Value
d_{hard}	8.94(m)
d_{soft}	13.52(m)
v_{soft}	3.73(m/s)
TTC_{soft}	3.62(sec)
TTC_{decel}	7.2(sec)

Table2. Values of human driving parameters

4.2. Driving Mode and Acceleration Decision

4.2.1. Acceleration of Each Mode

The acceleration that the vehicle should finally track is defined for each mode by applying the human driving parameters derived above. As mentioned in the section 4.1, there are two modes, which is soft mode and hard mode. The human driving parameters are the target state that the vehicle will track for each mode. Assuming constant deceleration, the longitudinal deceleration is simply defined depending on the target state of each mode and delay term.

In the soft mode, the target clearance and velocity is d_{soft} and v_{soft}, respectively. Also, the target clearance of the hard mode is d_{hard} with zero velocity.

$$a_{soft}(t) = -\frac{(v(t)^2 - v^2_{soft})}{2(d(t) - d_{soft} - v(t) \cdot T_{delay})} \tag{17}$$

$$a_{hard}(t) = -\frac{v(t)^2}{2(d(t) - d_{hard} - v(t) \cdot T_{delay})} \tag{18}$$

The final desired deceleration of the vehicle is determined as a minimum value of calculated decelerations for each of the N target pedestrians.

$$a_{desired} = \min(a_{ped[1]}, a_{ped[2]}, ..., a_{ped[N]}) \tag{19}$$

The mode is selected depending on relative distance, velocity and TTC between the ego vehicle and target pedestrian. Also, the criteria values are human driving

parameters mentioned in the section 4.2. The mode selection is visualized on the velocity and clearance plane, shown in the Fig.7. The cover region of the soft mode is defined by the conditions below.

4.2.2. Mode Selection

The mode is selected depending on relative distance, velocity and TTC between the ego vehicle and target pedestrian. Also, the criteria values are human driving parameters mentioned in the section 4.1.

The soft mode is a common situation when a target pedestrian is recognized from a sufficient distance to cope. Hence, the soft mode is limited to an area that can cope with a deceleration within $-2m/s^2$ in consideration of driving comfort [18]. Also, the human driving parameter TTC_{decel} is considered. The cover region of the soft mode can be expressed by equation (20).

$$0 \geq a_{soft}(t) \geq a_{\min} \quad and \quad TTC(t) \leq TTC_{decel} \tag{20}$$

The hard mode is a vehicle stop scenario and covers the region that soft mode cannot cope with. The area of hard mode is defined within a minimum coping distance in consideration of the delay. The cover region of the hard mode can be expressed by equation (21).

$$\begin{aligned} &d(t) \geq d_{hard} + v(t) \cdot t_{delay} \quad and \\ &TTC(t) \leq TTC_{decel} \,||\, d(t) \leq d_{soft} + v(t) \cdot t_{delay} \\ &except\ soft\ mode\ area \end{aligned} \tag{21}$$

The mode selection is visualized on the velocity and clearance plane, shown in the Fig.9.

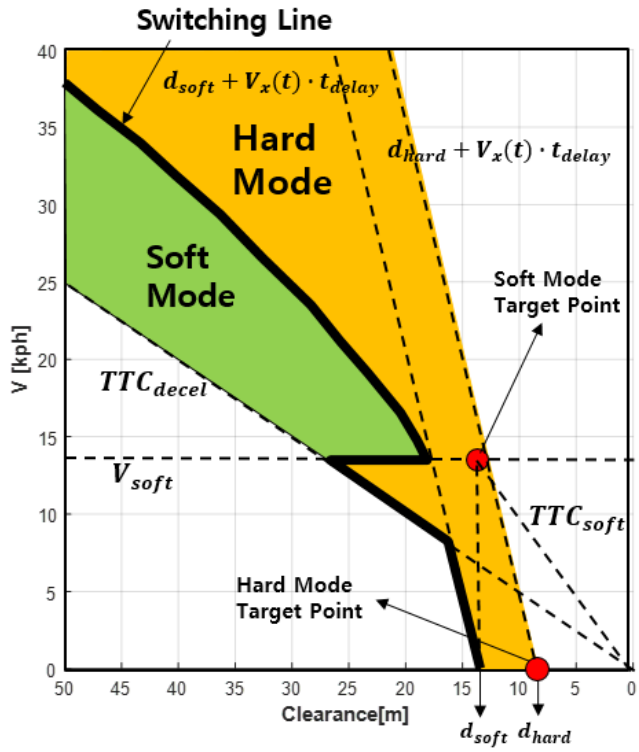

Fig. 9 Cover region of each mode in the longitudinal clearance-velocity plane

Chapter 5

Vehicle Test Result

5.1. Configuration of Experimental Vehicle

The experimental vehicle in this study is mainly equipped with Lidar sensors. The total detection sensor configuration is shown in Fig.10. The six IBEO Lidar sensors, front camera and around view monitoring(AVM) camera are mounted on the test vehicle. The Lidar sensors have four layers each with resolution of 5° and covers a 360 degree area around the ego vehicle. Also, the horizontal field of view(FOV) of each Lidar sensor is approximately 100m with $\pm 42.5^{\circ}$.

The test vehicle has also several actuator, controller and localization equipment, shown in Fig.11. The global states of the ego vehicle are from real-time-kinematic(RTK) global positioning system(GPS). In addition, the algorithm in this study is proceeded on the vehicle's pc and the desired acceleration as output is tracked through low level controller on the autobox and vehicle actuator. The autobox is rapid control prototyping(RCP) equipment.

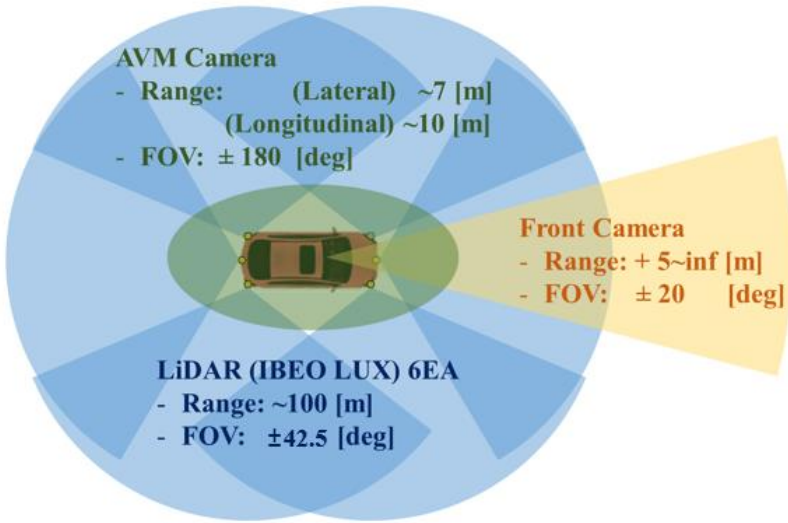

Fig. 10 Detection range for sensors installed in experimental vehicle

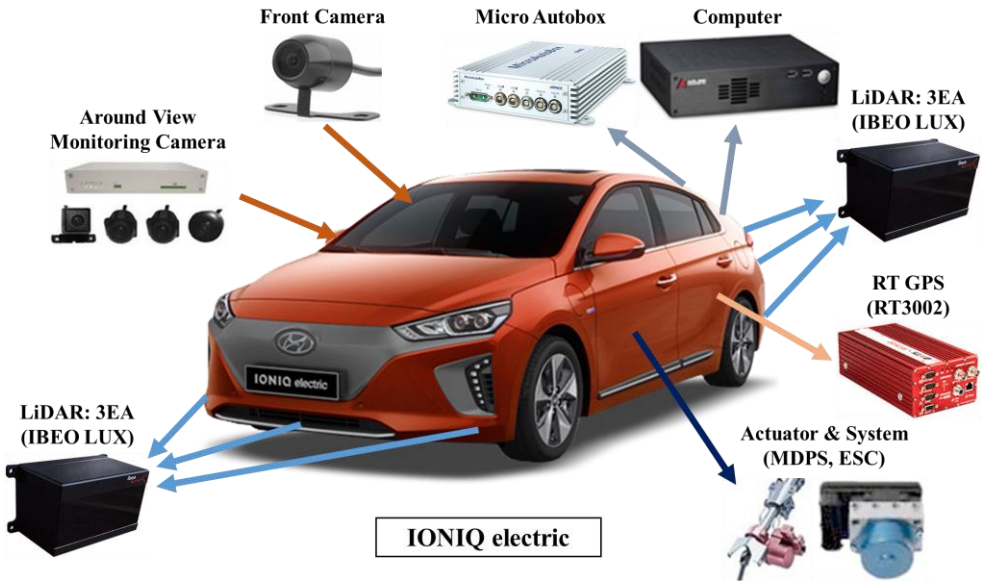

Fig. 11 Sensor configuration of experimental vehicle

5.2. Longitudinal Motion Planning for Pedestrian

The longitudinal motion planning of proposed algorithm is achieved by integrating all advanced processes such as probabilistic pedestrian yaw model, predicted trajectory and investigated human driving parameters. The algorithm is verified via repeated vehicle test on an unsignalized crosswalk at the Seoul National University. Two different scenarios are tested, and each test scenario involves three times of human driving and five times of autonomous driving for algorithm verification. The test environment is shown in the Fig.12 and the similarity with human driving is confirmed in both scenario. It means that the proposed pedestrian prediction model reflects human real-time prediction considering the uncertainty to cope with pedestrians. In other words, the probabilistic pedestrian yaw model is effective to use for vehicle's motion planning. Also, it is confirmed that the proposed driving mode decision and acceleration determination represent the human driving motion.

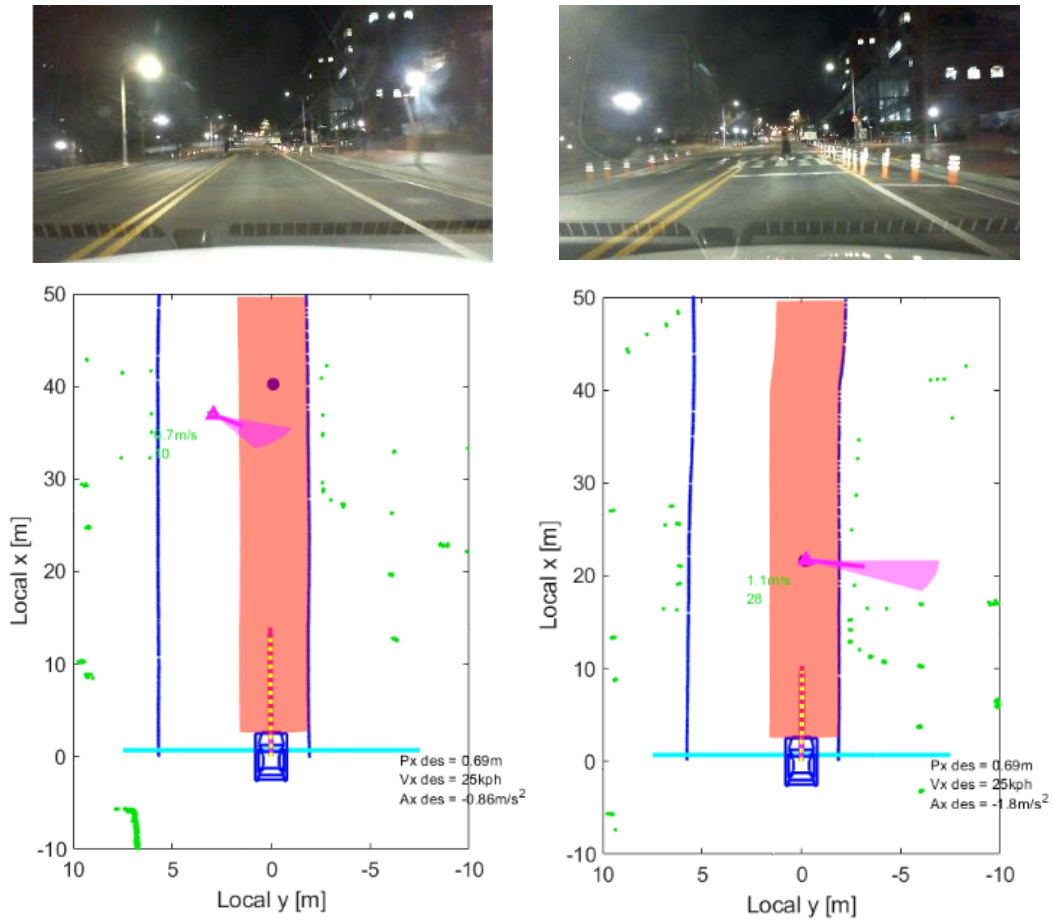

Fig. 12 Test environment and pedestrian model visualization

5.2.1. Soft Mode Scenario

The soft mode is a common situation in which the subject vehicle does not stop and smoothly decelerates to avoid collision with pedestrians. The motion of autonomous vehicle using proposed algorithm is compared to that of human driving in the same repetitive situation that the soft mode is selected. The motion similarity is verified by comparing the velocity profile and x and y clearance with a target pedestrian until the pedestrian completed the crossing, shown in the Fig.13-15. Also, the Fig.16 (a) and (b) indicate time series of the longitudinal clearance and velocity for one autonomous driving case in the soft mode. The Fig.16 (c) indicates the desired acceleration and actual acceleration profile with system delay for same driving case.

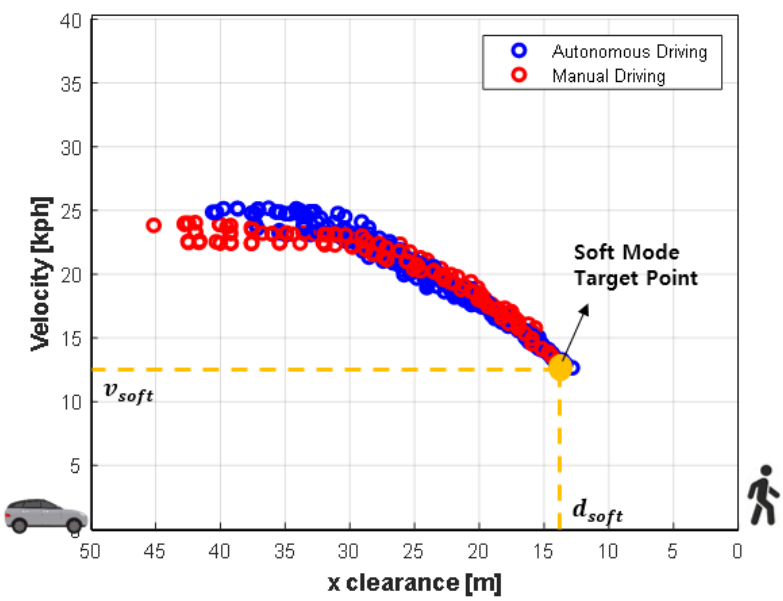

Fig. 13 Comparison of velocity profile for longitudinal clearance from the target pedestrian in the soft mode

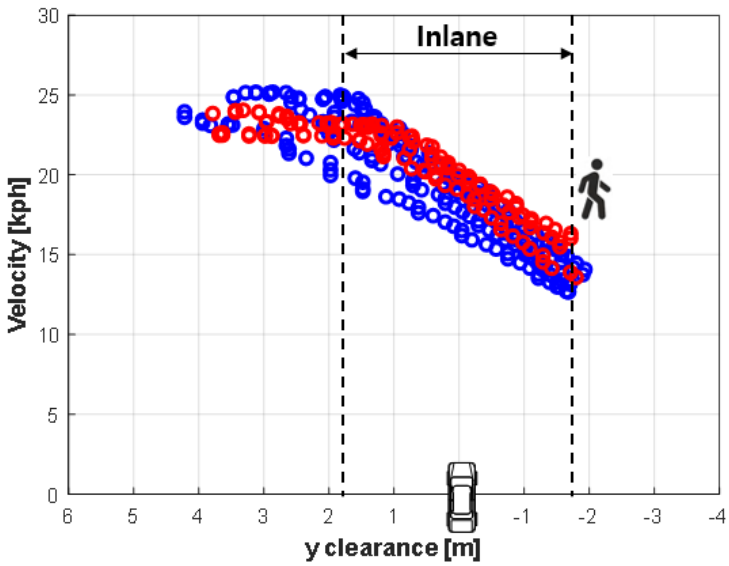

Fig. 14 Comparison of velocity profile for lateral clearance from the target pedestrian in the soft mode

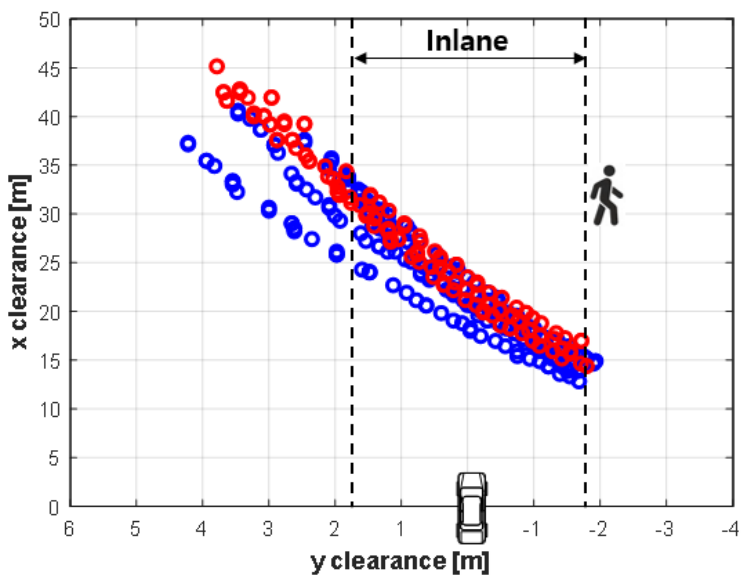

Fig. 15 Comparison of the lateral and longitudinal clearance from the target pedestrian on the two dimensional plane in the soft mode

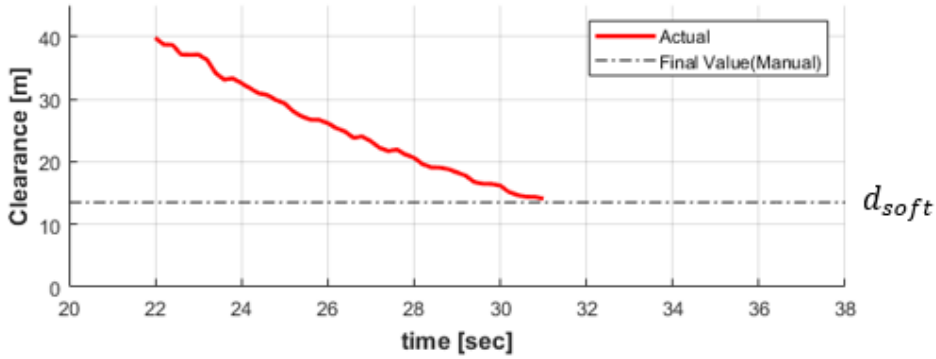

(a) Longitudinal clearance profile and target state

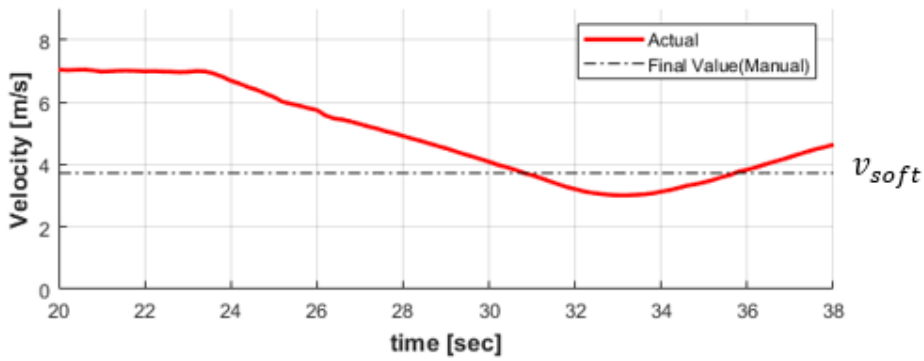

(b) Velocity profile and target state

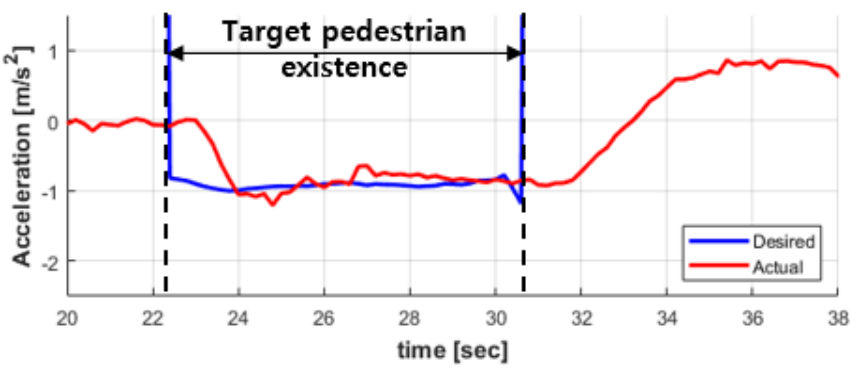

(c) Desired acceleration and actual acceleration profile in the soft mode

Fig. 16 States profile for an autonomous driving case in the soft mode

5.2.2. Hard Mode Scenario

In the hard mode, the acceleration is determined so that the vehicle stops in front of target pedestrian with a safe distance. As before, the motion of autonomous vehicle is compared to that of human driving in the same repetitive situation that the hard mode is selected. The motion similarity is verified by comparing the same variables in the soft mode and shown in the Fig.17-19. Also, the Fig.20 (a) and (b) indicate time series of the longitudinal clearance and velocity for one autonomous driving case in the hard mode. The Fig.20 (c) indicates the desired acceleration and actual acceleration profile with system delay for same driving case.

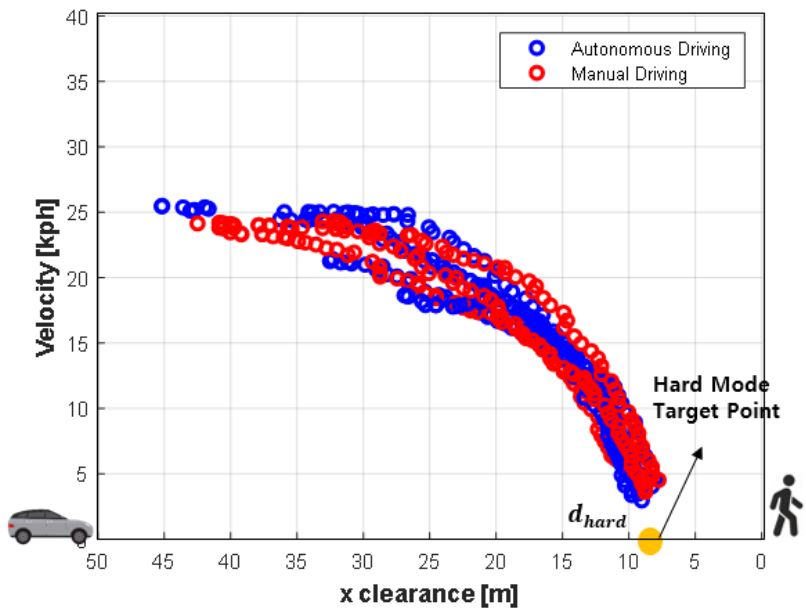

Fig. 17 Comparison of velocity profile for longitudinal clearance from the target pedestrian in the hard mode

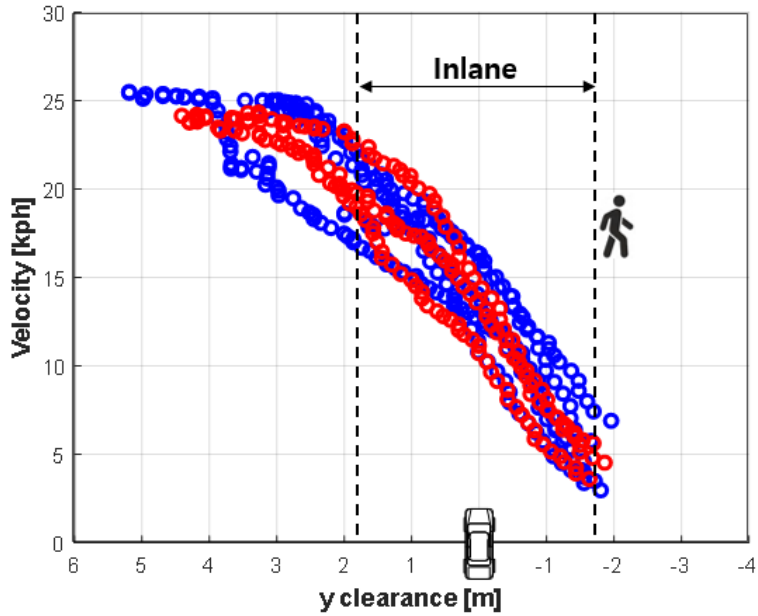

Fig. 18 Comparison of velocity profile for lateral clearance from the target pedestrian in the hard mode

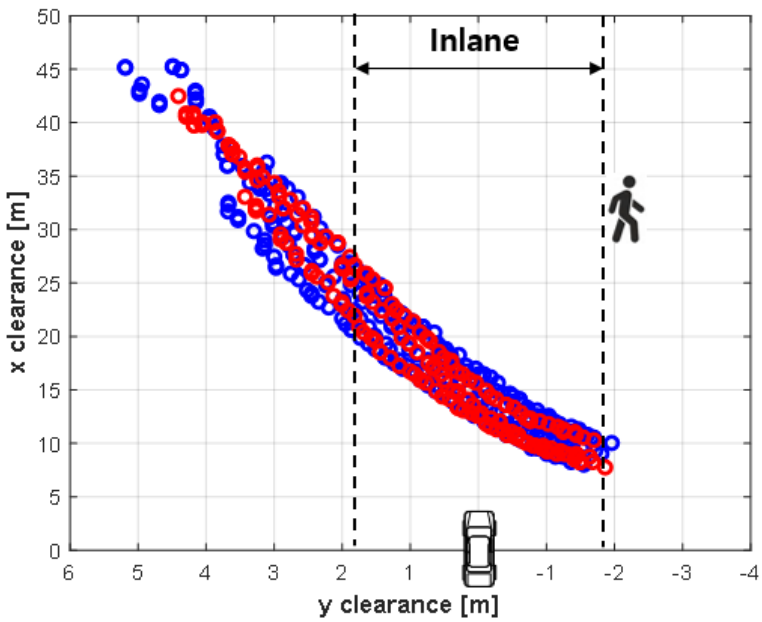

Fig. 19 Comparison of the lateral and longitudinal clearance from the target pedestrian on the two dimensional plane in the hard mode

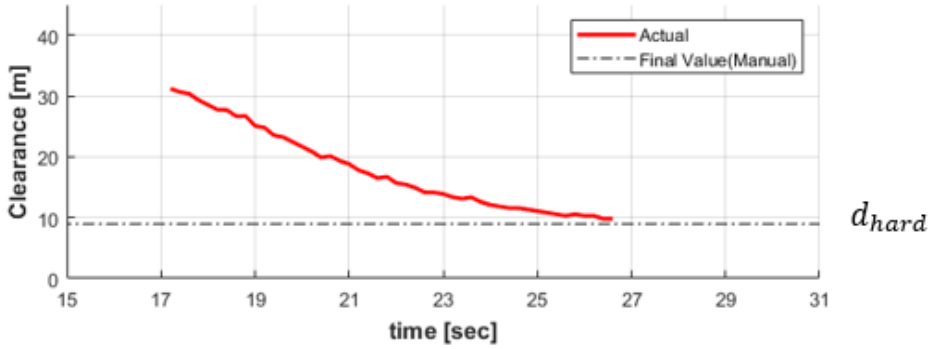

(a) Longitudinal clearance profile and target state

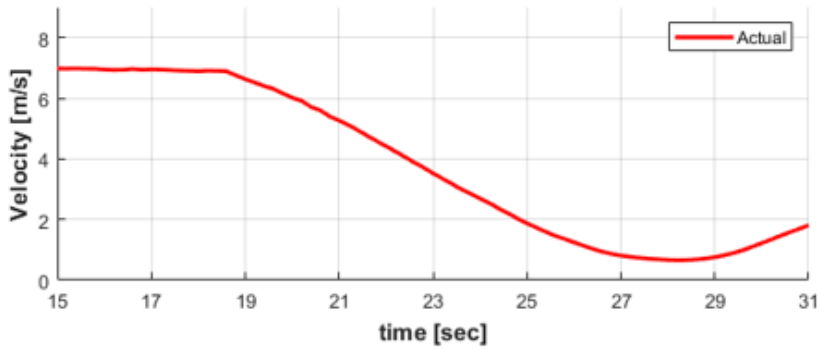

(b) Velocity profile and target state

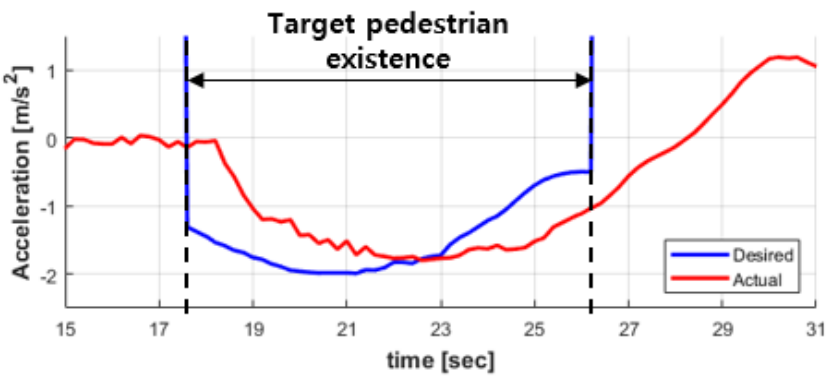

(c) Desired acceleration and actual acceleration profile in the soft mode

Fig. 20 States profile for an autonomous driving case in the hard mode

Chapter 6

Conclusion

In this study, a probabilistic pedestrian yaw model and longitudinal motion planning algorithm are mainly proposed using fundamental states information of pedestrian from Lidar sensor. To limit the area of future behavior considering the uncertainty in the direction of the pedestrian's behavior, the movement characteristics of pedestrian are analyzed and applied to define a probabilistic pedestrian yaw model. The movement data of pedestrians is collected using in-vehicle Lidar sensors and a total of 5000 step data sets are investigated. The defined correlation between pedestrian speed and yaw angle change is used to make an uncertain area of behavior for each pedestrian. Also, human driving parameters are investigated and applied to realize that the autonomous vehicle performs a human-like motion. The final motion planning is based on human driving parameters and pedestrian model.

The effectiveness of the proposed motion planning algorithm is evaluated via vehicle test. The autonomous driving is compared with human driving in the same pedestrian existence situation. As a results, the velocity and x, y clearance have similar profile with human driving in the repetitive tests. Therefore, the validity of the overall algorithm, such as pedestrian prediction considering behavior uncertainty, driving mode decision and acceleration determination is confirmed.

Bibliography

[1] Hashimoto, Y., Gu, Y., Hsu and Kamijo, S., “A Probabilistic Model for the Estimation of Pedestrian Crossing Behavior at Signalized Intersections”, IEEE 18th International Conference on Intelligent Transportation Systems, pp. 1520-1526, 2015.

[2] Hashimoto, Y., Gu, Y., Hsu, L. T., Iryo-Asano, M., & Kamijo, S., “A probabilistic model of pedestrian crossing behavior at signalized intersections for connected vehicles”, Transportation research part C: emerging technologies, 71, 164-181, 2016.

[3] Schneider N., Gavrila D.M., "Pedestrian Path Prediction with Recursive Bayesian Filters: A Comparative Study", German Conference on Pattern Recognition, Vol 8142, 2013.

[4] T. Fujioka, “Vehicle Following Control in Lateral Direction for Platooning,” Vehicle System Dynamics: International Journal of Vehicle Mechanics and Mobility, vol. 29, 1998.

[5] Simizu, Hiroaki, and Tomaso Poggio., “Direction estimation of pedestrian from images.”, MASSACHUSETTS INST OF TECH CAMBRIDGE ARTIFICIAL INTELLIGENCE LAB, 2003.

[6] Köhler, Sebastian, et al. "Early detection of the pedestrian's intention to cross the street." 2012 15th International IEEE Conference on Intelligent Transportation Systems. IEEE, 2012.

[7] Chen, Zhuo, Daniel CK Ngai, and N. H. C. Yung. "Pedestrian behavior prediction based on motion patterns for vehicle-to-pedestrian collision

avoidance." 2008 11th International IEEE Conference on Intelligent Transportation Systems. IEEE, 2008.

[8] Bertulis, T., Dulaski, D.M., "Driver Approach Speed and Its Impact on Driver Yielding to Pedestrian Behavior at Unsignalized Crosswalks", Journal of the Transportation Research Board, 2464. 46-51, 2014.

[9] Schneemann, F. and Gohl, I., "Analyzing driver-pedestrian interaction at crosswalks: A contribution to autonomous driving in urban environments", IEEE Intelligent Vehicles Symposium (IV), Gothenburg, pp. 38-43, 2016.

[10] Gu, Y., Hashimoto, Y., Hsu, L., Asano, M, Kamijo, S., “Human-like motion planning model for driving in signalized intersections.”, IATSS Research, Volume 41, Issue 3, pp. 129-139, 2017.

[11] Hsu, Y. C., Gopalswamy, S., Saripalli, S., & Shell, D. A, "An MDP Model of Vehicle-Pedestrian Interaction at an Unsignalized Intersection." 2018 IEEE 88th Vehicular Technology Conference (VTC-Fall). IEEE, 2018.

[12] Markkula, Gustav, et al. "Models of human decision-making as tools for estimating and optimizing impacts of vehicle automation." Transportation research record 2672.37 (2018): 153-163.

[13] Montufar, J., Arango, J., Porter, M., & Nakagawa, S, "Pedestrians' normal walking speed and speed when crossing a street." Transportation Research Record 2002.1 (2007): 90-97.

[14] Hamed Mohammed M., "Analysis of pedestrians’ behavior at pedestrian crossings." Safety science 38.1 (2001): 63-82.

[15] Keller, Christoph G., and Dariu M. Gavrila. "Will the pedestrian cross? a study on pedestrian path prediction." IEEE Transactions on Intelligent

Transportation Systems 15.2 (2013): 494-506.

[16] B. Kim and Yi, K., “Probabilistic states prediction algorithm using multi-sensor fusion and application to Smart Cruise Control systems”, IEEE Intelligent Vehicles Symposium, pp. 888-895, 2013.

[17] B. Kim, K. Yi, H. Yoo, H. Chong and B. Ko, "An IMM/EKF Approach for Enhanced Multitarget State Estimation for Application to Integrated Risk Management System," in IEEE Transactions on Vehicular Technology, vol. 64, no. 3, pp. 876-889, March 2015.

[18] Wu, Z., Liu, Y., & Pan, G., 2008, “A smart car control model for brake comfort based on car following”. IEEE transactions on intelligent transportation systems, 10(1), 42-46.

초 록

보행자 거동 및 운전자 주행 특성 기반의 자율주행 종방향 거동 계획

본 연구는 보행자의 미래 거동 방향에 대한 불확실성을 고려한 보행자 모델을 제안하고, 보행자 대응 시의 운전자 주행 특성을 반영하여 자율주행 차량의 종방향 모션을 계획하는 알고리즘을 제시한다. 도심 자율주행을 가능하게 하기위해서는 보행자와의 상호적인 주행이 필수적이다. 그러나, 보행자는 거동 방향 전환이 쉽게 일어나기 때문에 미래 거동을 예측하기가 어렵고, 이에 대응하는 자차의 거동을 결정짓는 데도 어려움이 있다. 이러한 보행자의 거동 불확실성이 존재함에도 자율 주행 차량이 보행자의 안전성을 확보하고 휴먼 운전자와 같이 거동하기 위해서는, 보행자의 거동 불확실성을 반영하는 보행자 모델이 우선적으로 필요하다.

해당 연구에서는 보행자 거동 특성을 조사하여 보행자 거동 확률 모델을 정의하고, 보행자 대응 상황에서의 운전자의 거동을 조사하여 자율주행 차량의 종방향 거동 계획에 적용한다. 해당 논문은 크게 보행자 모델 정의, 예측 기반 충돌 위험 평가 그리고 보행자 대응 종방향 거동 계획의 세 가지 주요 파트로 이루어져 있다. 첫 번째 파트에서 보행자 모델 정의의 핵심 이론은 보행자의 거동 속도와 방향을 전환하는 거동 사이에는 특정 상관관계를 가지고 있다는 것이다. 보행자의 거동 특성은 자율 주행 차량에 부착된 라이다 센서와 전방 카메라를 통해 획득한 보

행자 데이터를 통계적으로 분석한 결과로 도출되었다. 해당 데이터를 통해 속도에 따라 보행자가 모든 방향에 대해서 거동할 확률이 도출되고, 보행자의 미래 거동 범위는 도출된 확률 분포에서 유효 시그마 범위를 설정하여 구획된다. 이는 보행자가 일정 시간 동안 특정 확률로 거동할 영역을 고려하여, 위험이 존재할 수 있는 보행자에 대해서 미리 차량의 움직임을 계획할 수 있도록 한다. 두 번째 파트로 보행자와 자 차량의 일정 시간 동안의 위치 정보를 예측하여 충돌 위험성을 평가한다. 보행자 예측은 앞서 도출한 보행자 유효 예측 거동 범위 내에서 가장 위험성이 큰 방향으로 움직인다고 가정한다. 또한, 자 차량의 경우 주어진 로컬 경로를 따라 움직인다는 가정을 하는 차선 유지 모델을 사용한다. 예측 결과를 통해 현재 추가적인 감속도를 가하지 않았을 때, 충돌 위험이 존재하는지 확인한다. 마지막으로, 타겟이 되는 보행자에 대한 종방향 거동을 결정한다. 우선적으로 보행자 대응 상황에서 적절한 감속도와 감속 시점을 결정하기 위해 휴먼 운전자 주행 데이터를 분석한다. 이를 통해 주행에서 핵심적인 파라미터들이 정의되고, 해당 파라미터들은 종방향 거동 계획에 반영된다. 따라서 최종적으로 보행자 예측 거동 영역에 대해서 자율 주행 차량의 추종 가속도이 결정된다.

제시된 알고리즘은 실차 테스트를 통해 성능이 확인된다. 테스트 결과, 도출한 보행자 모델과 예측 모델을 바탕으로 한 감속 결정 시점과 감속도의 궤적이 동일 상황들에 대해서 능숙한 운전자와 유사함이 확인되었다.

주요어: 자율주행, 종방향 거동 계획, 보행자 확률 모델, 인간 유사 거동
학　　번: 2018-20946